JCB Article

Interference with the cytoplasmic tail of gp210 disrupts "close apposition" of nuclear membranes and blocks nuclear pore dilation

Sheona P. Drummond and Katherine L. Wilson

Department of Cell Biology, Johns Hopkins University School of Medicine, Baltimore, MD 21205

We tested the hypothesis that gp210, an integral membrane protein of nuclear pore complexes (NPCs), mediates nuclear pore formation. Gp210 has a large lumenal domain and small COOH-terminal tail exposed to the cytoplasm. We studied the exposed tail. We added recombinant tail polypeptides to *Xenopus* nuclear assembly extracts, or inhibited endogenous gp210 tails using anti-tail antibodies. Both strategies had no effect on the formation of fused flattened nuclear membranes, but blocked NPC assembly and nuclear growth. Inhibited nuclei accumulated gp210 and some nucleoporin p62, but failed to incorporate nup214/CAN, nup153, or nup98 and were defective for nuclear import of lamin B3. Scanning and transmission EM revealed a lack of "closely apposed" inner and outer membranes, and the accumulation of novel arrested structures including "mini-pores." We conclude that gp210 has early roles in nuclear pore formation, and that pore dilation is mediated by gp210 and its tail-binding partner(s). We propose that membrane fusion and pore dilation are coupled, acting as a mechanism to control nuclear pore size.

Introduction

The eukaryotic genome is enclosed by two nuclear membranes. A mechanism for fusion between the inner and outer membranes to generate pores is essential for the genome to communicate with the cytoplasm; indeed, the evolution of eukaryotic organisms probably depended on a "porogenic" fusion mechanism. Assembling pores have diameters that range from 6–40 nm (Goldberg et al., 1997). In vertebrates, mature pores have a diameter of ~50–70 nm and are occupied by nuclear pore complexes (NPCs),* which regulate molecular traffic between the nucleoplasm and cytoplasm (Bayliss et al., 2000; Wente, 2000; Yoneda, 2000). Vertebrate NPCs have a maximum mass of 125 MD (Reichelt et al., 1990; Panté and Aebi, 1994) and consist of multiple copies of ~40 distinct proteins (Miller and Forbes, 2000), termed nucleoporins. NPCs are anchored at the pore membrane domain, where the inner and outer membranes merge. Soluble nucleoporins are recruited to the pore membrane during NPC assembly. Pore formation was proposed to be triggered by the binding of soluble proteins to membranes (Fabergé, 1974) or by chromatin-induced indentations of the inner nuclear membrane, as seen by transmission EM (TEM; Maul et al., 1971). A role for chromatin in the formation of mature functional NPCs is likely, even though chromatin is not essential for porogenic membrane fusion per se (Maul, 1977; Vasu and Forbes, 2001). Unidentified soluble nucleoporins are required to stimulate pore formation in regions of flattened nuclear membranes (Macaulay and Forbes, 1996), and also in ER-like membranes known as annulate lamellae, which lack chromatin (Dabauvalle et al., 1991; Meier et al., 1995). Along with most aspects of NPC assembly, the mechanism of porogenic membrane fusion is an important open question in biology.

Membrane fusion is central to secretion, endocytosis, and the biogenesis of the ER, Golgi apparatus, and mitochondria (Bennet and Scheller, 1993). These fusions are mediated by cytosolic proteins that first disrupt the cytosolic leaflet of each bilayer (Robinson and Martin, 1998). In contrast, nuclear pore fusion involves the lumenal leaflets of the nuclear inner and outer membranes, and therefore probably involves pro-

The online version of this article includes supplemental material.

Address correspondence to Katherine L. Wilson, Department of Cell Biology, WBSB Room G10, Johns Hopkins University School of Medicine, 725 N. Wolfe Street, Baltimore, MD 21205. Tel.: (410) 955-1801. Fax: (410) 955-4129. E-mail: klwilson@jhmi.edu

S.P. Drummond's present address is Department of Structural Cell Biology, Paterson Institute for Cancer Research, Christie Hospital, Wilmslow Road, Manchester M20 9BX, UK.

*Abbreviations used in this paper: GST, glutathione-*S*-transferase; HA, hemagglutinin; NIB, nuclear isolation buffer; NPC, nuclear pore complex; SEM, scanning EM; TEM, transmission EM.

Key words: nucleus; membrane fusion; *Xenopus* egg extracts; nuclear pore complex; nucleoporin

teins within the lumenal space. Viral fusogens, such as hemagglutinin (HA) protein of influenza virus (Skehel and Wiley, 2000), are viewed as possible models for lumenal membrane fusion events in normal cells. At low pH, membrane-embedded HA trimers undergo a conformational change that exposes their fusogenic peptides, allowing them to destabilize the opposing lipid bilayer and sequentially trigger membrane hemifusion, pore formation, and pore dilation (Hernandez et al., 1996; Kozerski et al., 2000). A conceptually different possibility is that soluble nucleoporins might assemble on the chromatin surface and then recruit surrounding membranes laterally as membranes attach to chromatin during nuclear assembly. However, this hypothetical mechanism is restricted; it could function only during the few minutes in telophase before chromatin is enclosed by membranes, it cannot explain pore formation during G1, S, or G2 phases of the vertebrate cell cycle, nor explain pore formation in eukaryotes (e.g., *Saccharomyces cerevisiae*) whose nuclei remain intact during mitosis.

Wozniak et al. (1989) and Greber et al. (1990) proposed that nuclear pore formation might be mediated by gp210, an integral membrane protein found at pores (Gerace et al., 1982). Gp210 is linked structurally to NPCs, as antibodies that target lumenal epitopes of gp210 decrease both active and passive transport through NPCs (Greber and Gerace, 1992). The majority of gp210 (95% of its mass) lies within the nuclear envelope lumen, but its short COOH-terminal tail is exposed to the cytosol (Greber et al., 1990). This cytoplasmic tail is specifically phosphorylated during mitosis, presumably to facilitate NPC disassembly (Favreau et al., 1996). Circumstantial evidence for gp210 as a fusogen came from topological studies. Rat gp210 was predicted by hydropathy analysis to have two membrane spanning domains (Wozniak and Blobel, 1992). However, topological studies showed that only one, the COOH-terminal hydrophobic domain, actually spans the membrane, whereas the other sits in the lumenal domain (Greber et al., 1990). Wozniak and Blobel (1992) suggested that this "extra" hydrophobic domain might destabilize lipid bilayers, triggering fusion. Also analogous to HA, which forms trimers, gp210 was calculated to form dimers or trimers (Gerace et al., 1982). Recent cross-linking studies show that gp210 forms stable dimers (Favreau et al., 2001).

By indirect immunofluorescence, many soluble nucleoporins reaccumulate rapidly at assembling nuclear envelopes (Chaudhary and Courvalin, 1993; Bodoor et al., 1999; Haraguchi et al., 2000). In contrast, gp210 is detectable at early stages of nuclear assembly, but most gp210 does not reaccumulate until late telophase or early G1 (Chaudhary and Courvalin, 1993; Bodoor et al., 1999). Note that gp210 is not excluded from nuclei at early stages of assembly; rather, it simply reaccumulates slowly, raising questions about its theoretical early role in pore formation. The only other known integral membrane nucleoporin in vertebrates, POM121, accumulates rapidly during nuclear assembly (Bodoor et al., 1999; Daigle et al., 2001). POM121 has a large exposed domain and a small lumenal domain (Soderqvist and Hallberg, 1994). Overexpression of POM121 in mammalian cells causes NPCs to form and accumulate in ER membranes, suggesting direct or indirect roles in triggering NPC formation (Imreh and Hallberg, 2000). In yeast, overexpression of a soluble nucleoporin named nup53, which has an amphipathic α-helix, induces the formation of nuclear inner membrane tubules with empty pores (Marelli et al., 2001).

We used *Xenopus* extracts to directly test the role of gp210, if any, in pore formation. *Xenopus* egg extracts are a powerful and well-characterized system for studying nuclear pore formation (Miller and Forbes, 2000; Vasu and Forbes, 2001). We focused on the small exposed tail of gp210, because it is freely accessible to reagents added to cell-free extracts. We found that a recombinant gp210 tail polypeptide and antibodies against the exposed COOH-terminal tail of *Xenopus* gp210 both inhibited pore formation. The arrest morphologies suggest an unanticipated direct function for the gp210 tail and its binding partners in the dilation of nascent nuclear pores.

Results

To study gp210 function in the *Xenopus* system, we first had to identify *Xenopus* gp210. We identified a partial cDNA corresponding to the COOH terminus of *Xenopus* gp210 by using the rat gp210 sequence to search the *Xenopus* EST database (see Materials and methods; this EST clone had a mutation). We then generated the corresponding wild-type PCR product from a *Xenopus* oocyte cDNA library. This partial cDNA encoded a polypeptide of 251 residues that was 39% identical and 47% similar to the COOH-terminal

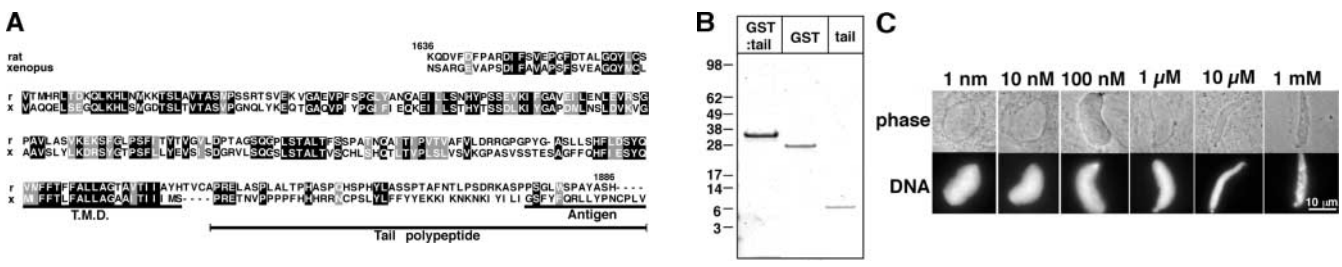

Figure 1. **Partial *Xenopus* gp210 sequence and purification and testing of gp210 tail polypeptide.** (A) Sequence alignment of rat gp210 (residues 1636–1886) and the 251-residue polypeptide encoded by the partial *Xenopus* cDNA. The transmembrane domain (TMD) and the 16-residue peptide (antigen) used to generate rabbit serum 3860 are underlined. Also indicated is the tail polypeptide of *Xenopus* gp210 that was recombinantly expressed, purified, and used to inhibit nuclear assembly. (B) SDS-PAGE gel showing the GST–gp210 tail fusion protein before (GST:tail) and after (GST, tail) cleavage by thrombin (see Materials and methods). (C) Effects of purified gp210 tail on nuclear assembly in *Xenopus* egg extracts. Purified gp210 tail was added to nuclear assembly reactions (final concentrations indicated) at time zero. 2 h later, nuclei were visualized by phase contrast microscopy and Hoescht staining for DNA. Bar, 10 μm.

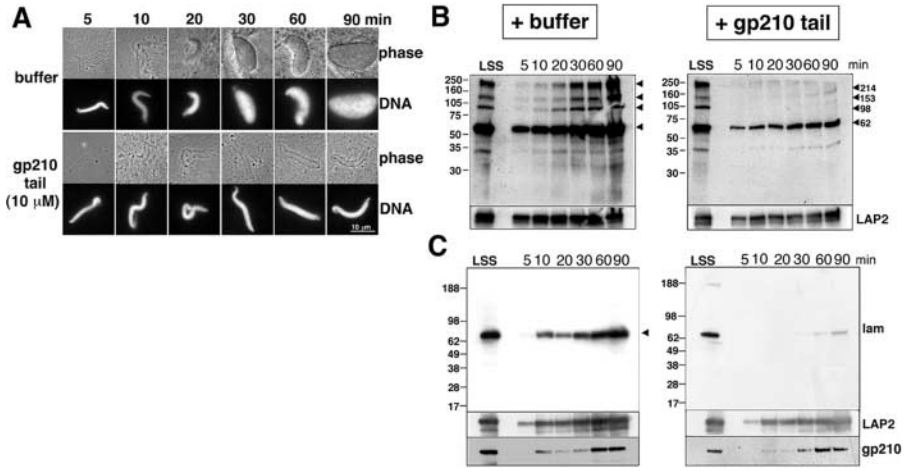

Figure 2. **Purified gp210 tail polypeptide inhibits nuclear growth and NPC assembly.** (A) Time course of nuclear assembly in the presence of 10 μM tail polypeptide. Nuclei were assembled in the presence (10 μM) or absence (buffer control) of purified gp210 tail. Aliquots were removed at the times indicated and imaged by phase contrast microscopy to visualize nuclear membranes, and by fluorescence microscopy to visualize Hoescht-stained DNA. Bar, 10 μm. (B and C) Western blot analysis of tail-inhibited nuclei. Nuclei assembled in the presence of buffer or 10 μM gp210 tail were isolated after 5, 10, 20, 30, 60, and 90 min of assembly, run on SDS-PAGE, blotted, and probed with (B) mAb 414 to identify incorporated FG repeat nucleoporins, and (C) mAb S49F to detect lamin B3. Each blot was stripped and reprobed with antibodies against *Xenopus* LAP2 to confirm recruitment of nuclear-specific membranes (bottom). The blots in (C) were lastly restripped and probed with antibodies against gp210 (bottom). Lanes marked LSS (low speed supernatant) were loaded with 1 μl of crude *Xenopus* egg extract.

251 residues of rat gp210 (Fig. 1 A). As shown below, antibodies against the COOH terminus confirmed that this cDNA encoded gp210.

Recombinant gp210 tail polypeptide inhibits nuclear growth

We hypothesized that the function of gp210 may require interactions between its cytoplasmic tail and other nucleoporins. To test this hypothesis, we first expressed the 61-residue gp210 tail as a 32.8-kD fusion protein with glutathione-*S*-transferase (GST), from which the 6.8-kD tail was purified after cleavage by biotinylated thrombin (Fig. 1 B). The purified gp210 tail was added, at time zero, to nuclear assembly reactions consisting of reconstituted *Xenopus* egg cytosol and membranes plus demembranated sperm chromatin (Lohka and Masui, 1984; Newmeyer and Wilson, 1991). Purified gp210 tail was added to final concentrations ranging from 1 nM to 1 mM. Nuclei were allowed to assemble for 90 min and then examined by light microscopy (Fig. 1 C). Nuclear growth was fully inhibited by tail concentrations of 10 μM or more. The growth-inhibited nuclei had phase-dense membranes at the chromatin surface, but failed to expand or decondense the chromatin. Inhibition by exogenous gp210 tails was specific, because control nuclei assembled in the presence of an unrelated polypeptide (thrombin-cleaved, purified 10 μM GST) assembled and grew normally (unpublished data). Further experiments were done using the tail polypeptide at 10 μM, the lowest concentration tested that terminally arrested nuclear envelope growth. This represented a fivefold excess over endogenous gp210 (~2 μM), as estimated from densitometry analysis of immunoblots of *Xenopus* membrane proteins and known concentrations of the recombinant *Xenopus* gp210 tail (unpublished data).

To determine the time course of inhibition, reactions were supplemented at time zero with 10 μM gp210 tail (or buffer control) and imaged after 5, 10, 20, 30, 60, and 90 min of assembly (Fig. 2 A). Membrane recruitment to the chromatin surface was neither delayed nor inhibited by exogenous gp210 tails. However, defects in nuclear growth and chromatin decondensation were obvious within 20–30 min, when buffer addition control nuclei became fully enclosed by a nuclear envelope and began enlarging. Nuclear growth requires functional NPCs and active nucleocytoplasmic transport (Macaulay and Forbes, 1996; Wiese et al., 1997). The growth arrest caused by exogenous gp210 tails suggested defects in NPC assembly or function.

Gp210 tail-inhibited nuclei fail to incorporate nucleoporins and lack lamin B3

To determine if tail-inhibited nuclei were defective for NPC assembly or nuclear import, we tested the incorporation of FG-repeat nucleoporins using mAb 414, and tested the accumulation of lamin B3, which depends on signal-mediated nuclear import (Loewinger and McKeon, 1988; Meier et al., 1991; Firmbach-Kraft and Stick, 1995). Aliquots were removed from assembly reactions after incubating for 5, 10, 20, 30, 60, and 90 min, and the nuclei were purified (see Materials and methods), resolved by SDS-PAGE, blotted, and probed for either nucleoporins (Fig. 2 B) or lamin B3 (Fig. 2 C) using mAb 414 and mAb S49F, respectively. The corresponding control and inhibited samples were processed for Western blotting in pairs so that the signals were directly comparable in qualitative terms. As a further control, blots were stripped and reprobed with an antibody that recognizes nuclear membrane LAP2 proteins (Fig. 2, B and C, bottom), or an antibody against *Xenopus* gp210 (Fig. 2 C, bottom; this antibody is described below). These experiments confirmed that nuclear membranes were recruited to chromatin. Several isoforms of LAP2 were detected, as expected (Gant et al., 1999). The reduced signals for both LAP2 and gp210 in inhibited nuclei were consistent with their smaller surface areas. Interestingly, the gp210 blots showed that gp210 accumulated over time in both the control and inhibited nuclei (Fig. 2 C), demonstrating that gp210 can accumulate in nuclei that lack at least a subset of soluble nucleoporins.

mAb 414 recognizes five nucleoporins (nup358, nup214/CAN, nup153, nup98, and p62), all of which carry the *O*-linked *N*-acetylglucosamine modification (Davis and Blobel, 1987; Aris and Blobel, 1989; Shah and Forbes, 1998). Nup358 was not detected by mAb 414 in our Western blots,

presumably because it failed to transfer under our conditions. The other four nucleoporins accumulated rapidly over time in the positive control nuclei (Fig. 2 B, buffer), as expected. The tail-inhibited nuclei acquired p62, although not to control levels (Fig. 2 B, gp210 tail). Tail-inhibited nuclei appeared to be depleted of nup214, nup153, and nup98, despite near-normal accumulation of gp210 in these nuclei (Fig. 2 C).

These results suggested that gp210 tail polypeptides selectively blocked the recruitment of several soluble nucleoporins, but not gp210 itself. Nup214 normally localizes to NPC cytoplasmic filaments (Kraemer et al., 1994), whereas nup153 and nup98 localize to the NPC basket and proposed intranuclear filaments (Sukegawa and Blobel, 1993; Radu et al., 1995; Fontoura et al., 2001). Our conclusion that NPC assembly was blocked in tail-inhibited nuclei was independently supported by the greatly reduced import of lamin B (Fig. 2 C). To explain these defects, we hypothesized that our recombinant tail polypeptides competed for putative tail-binding nucleoporins, which could be either soluble or membrane associated. Our results thus implicate a putative gp210 tail–binding nucleoporin(s) as having an early role in NPC assembly.

Antibodies to the gp210 tail also arrest nuclear growth

We raised rabbit polyclonal antibodies against the predicted COOH-terminal 16 residues of *Xenopus* gp210 (Fig. 1 A, underlined). This serum (no. 3860) was used to probe immunoblots of *Xenopus* egg membrane and cytosol fractions. The immune antibodies specifically recognized a membrane protein that migrated on SDS gels at ~195 kD (Fig. 3 A), similar to the antigen recognized by a proposed anti-*Xenopus* gp210 monoclonal antibody (Gajewski et al., 1996). Our 195-kD antigen was undetectable in the cytosolic fraction, as expected for an integral membrane protein. Recognition of the 195-kD membrane protein was specifically competed by pretreating serum 3860 with the peptide antigen (Fig. 3 A, +). When used for indirect immunofluorescence of cultured *Xenopus* epithelial (A6) cells, immune (but not preimmune) serum 3860 specifically stained the nuclear envelope in a punctate pattern (Fig. 3 B, Xgp210) that colocalized with the family of FG repeat nucleoporins recognized by monoclonal antibody 414 (Fig. 3 B, nups). Punctate nuclear envelope staining was also seen in nuclei assembled in *Xenopus* extracts (unpublished data). The homology, appropriate antigen size on gels, membrane cofractionation, and colocalization with NPCs at the nuclear envelope all verified that clone AW642061 represents *Xenopus* gp210, and further showed that our antibodies specifically recognized *Xenopus* gp210.

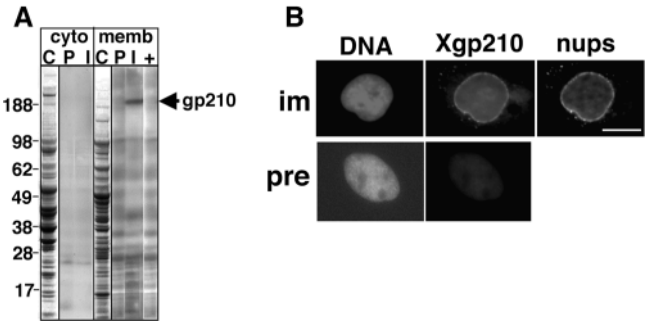

Figure 3. **Polyclonal anti–tail peptide serum 3860 recognizes a 195-kD membrane protein that colocalizes with NPCs.** (A) SDS-PAGE of *Xenopus* egg cytosol (cyto) and membrane (memb) proteins stained with Coomassie blue (C) or transferred to polyvinylidene difluoride membrane and probed with preimmune serum (P), immune serum (I), or peptide-blocked immune serum (+). (B) Immunofluorescence of *Xenopus* A6 cells stained with Hoescht to localize DNA, mAb 414 to localize NPCs, and either preimmune (pre) or immune (im) serum 3860 against Xgp210. Bar, 10 μm.

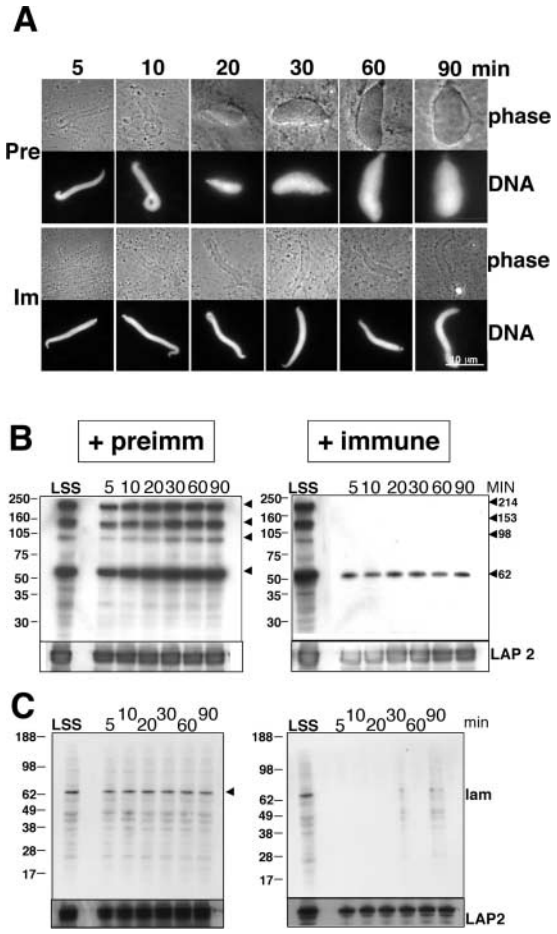

Figure 4. **Antibodies to the gp210 tail inhibit nuclear growth.** (A) Nuclei were assembled in the presence of immune or preimmune serum 3860 antibodies against the gp210 tail (see Materials and methods). Aliquots were removed at the times indicated, fixed, and visualized by phase contrast microscopy to show membranes and fluorescence microscopy to show Hoescht-stained DNA. Bar, 10 μm. (B and C) Western blot analysis of antibody-inhibited nuclei. Nuclei assembled in the presence of preimmune or immune serum 3860 were isolated after 5, 10, 20, 30, 60, and 90 min of incubation, run on SDS-PAGE, blotted, and probed with (B) mAb 414 to identify incorporated FG repeat nucleoporins and (C) mAb S49F to detect lamin B3. Each blot was stripped and reprobed with antibodies against *Xenopus* LAP2 to confirm the recruitment of nuclear-specific membranes (bottom).

To independently inhibit gp210 tail function, we assembled nuclei in the presence of serum 3860 antibodies, which were predicted to bind the COOH-terminal tip of the endogenous gp210 tail. Immune or preimmune antibodies were added at time zero to nuclear assembly reactions, and assembly was monitored at different times by light microscopy (Fig. 4 A). Nuclei assembled in the presence of immune antibodies successfully recruited membranes, but the chro-

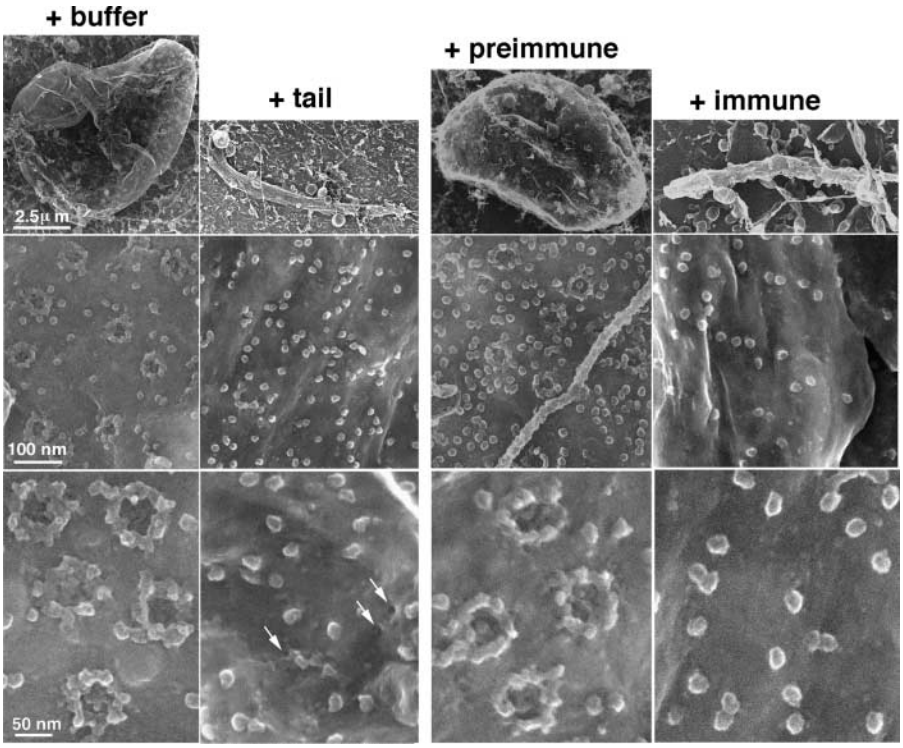

Figure 5. **SEM of tail- and antibody-inhibited nuclei coated with a 2.5-nm layer of chromium.** Top row shows nuclei at low magnification to demonstrate the growth arrest caused by exogenous gp210 tails and immune antiserum. (Left) Nuclei were assembled for 2 h in the presence of buffer (+ buffer) or 10 μM purified gp210 tail (+ tail). Control nuclei were enclosed by flattened membranes with mature NPCs, best seen at higher magnification in the bottom. Nuclei assembled with 10 μM gp210 tails were enclosed by fused and flattened nuclear membranes that lacked mature NPCs, but did have tiny pores (+ tail, bottom, arrows). (Right) Nuclei were assembled with either preimmune (+ preimmune) or immune (+ immune) antisera against the gp210 tail. Preimmune-treated control nuclei had typical nuclear envelopes and NPCs (+ preimmune, bottom). Nuclei assembled with immune antibodies were enclosed by flattened membranes that lacked any surface-detectable pore-related structures. Scale bars (left) apply to each row.

matin failed to decondense and a block to nuclear envelope growth was obvious by the 20-min time point (Fig. 4 A, Im). By light microscopy, the arrested phenotype was indistinguishable from that caused by recombinant gp210 tails.

Nuclei assembled in the presence of preimmune or immune antibodies were isolated, processed for SDS-PAGE, and immunoblotted in pairs (control and inhibited) for the incorporation of mAb 414–reactive nucleoporins and lamin B3 (Fig. 4, B and C). Similar to tail-inhibited nuclei, the antibody-inhibited nuclei incorporated detectable levels of only one FG repeat nucleoporin, p62 (Fig. 4 B), and failed to accumulate lamin B3 (Fig. 4 C), consistent with an early arrest of NPC assembly and lack of nuclear transport activity.

Tail- and antibody-inhibited nuclei are enclosed by flattened nuclear membranes

The above results suggest that exogenous tail peptides and gp210 antibodies both arrested nuclear assembly at a very early stage, with membranes attached to chromatin but no functional pores. Nuclear pore formation and NPC assembly can be assayed by scanning EM (SEM) as soon as patches of nuclear membranes flatten onto the chromatin surface (Wiese et al., 1997). In wild-type reactions, pores form asynchronously and rapidly, and many mature NPCs are already present by ~30 min, when chromatin becomes enclosed by nuclear membranes (Wiese et al., 1997). To determine if our inhibitors disrupted these cytosol-dependent membrane fusion events, we imaged the inhibited and control nuclei (assembled for 2 h) by SEM (see Materials and methods). SEM visualization of control nuclei, assembled in the presence of buffer or preimmune serum, showed full-size nuclei with fused and flattened nuclear envelopes and mature NPCs, as expected (Fig. 5). Nuclei assembled with either gp210 tail polypeptides or anti-tail antibodies were growth arrested (Fig. 5, top), consistent with our light microscopy results, and were all enclosed by flattened and fused membranes, showing that nuclear vesicles fused normally. Importantly, these arrested nuclei lacked NPCs (Fig. 5; center and bottom). However, tiny dimples or holes with diameters of 3–7 nm were visible on the surface of tail-inhibited nuclei (Fig. 5, + tail, arrows in bottom panel). These tiny holes were scarce in the antibody-arrested nuclei. We concluded that our inhibitors arrested nuclear pore formation at two distinct stages, with tail polypeptides arresting after the formation of mini-pores. Antibodies against the gp210 tail appeared to arrest pore formation at an earlier stage.

TEM reveals novel arrested intermediates in pore formation

We next used TEM to visualize the arrested nuclear membranes in cross section (see Materials and methods). Positive control nuclei assembled in the presence of buffer (Fig. 6 A) or preimmune serum (Fig. 6 E) formed nuclear envelopes with mature NPCs, as expected. The membranes surrounding a mature NPC are shown (tangential section) and traced in Fig. 6, I and J. In contrast, nuclei arrested by the competing tail polypeptides (Fig. 6, B–D) or anti-gp210 antibodies (Fig. 6, F–H) had striking, unprecedented morphologies: the inner and outer membranes appeared to be fused at frequent intervals, forming discrete electron-dense foci (Fig. 6, B and F, arrows). In the mini-pores produced by exogenous tail polypeptides, the two membranes were almost parallel on an axis perpendicular to the nuclear envelope, and were separated by a gap of 1–5 nm (Fig. 6, C and D). Tracings of the membrane edge suggested that in two of three arrested structures shown, membrane fusion might have been completed to yield a narrow (1–5 nm) pore (Fig. 6 D, white dotted lines). Holes in this size range were barely detectable in

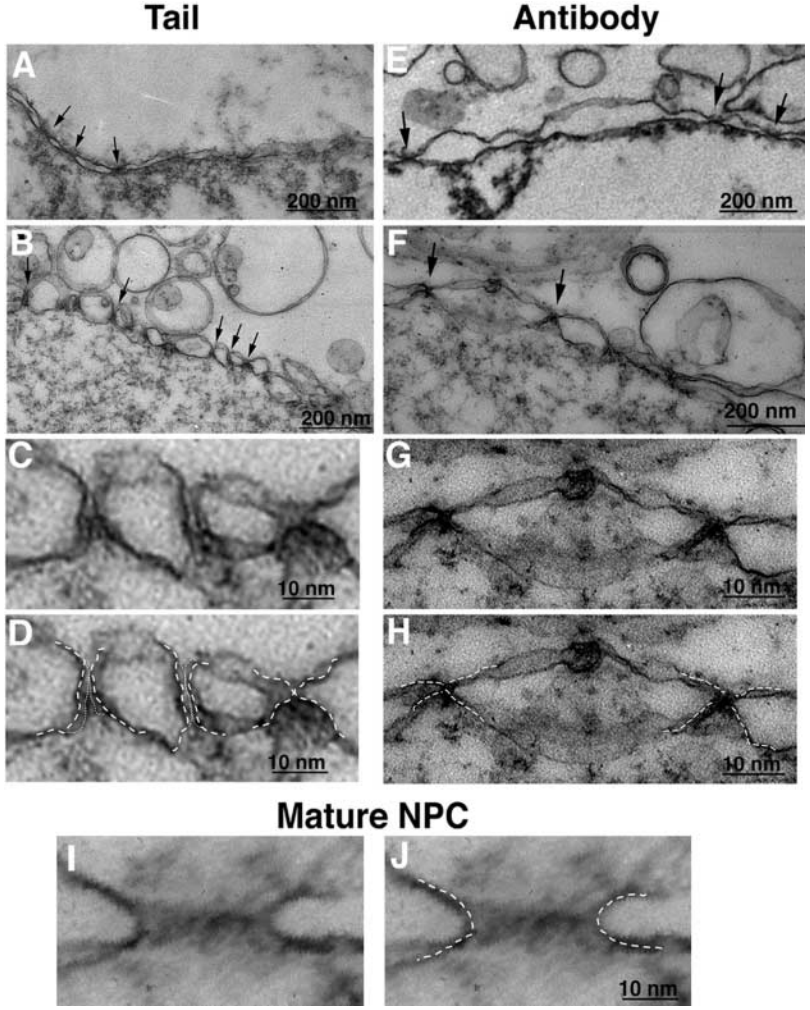

Figure 6. **TEM of tail- and antibody-inhibited nuclei.** Nuclei were assembled for 2 h in the presence of (A) buffer alone or (B, C, and D) 10 μM purified gp210 tail polypeptides. Control nuclei had decondensed chromatin enclosed within a typical flattened nuclear envelope with NPCs (arrows). Nuclear membranes assembled in the presence of 10 μM gp210 tail (B–D) accumulated novel arrested structures (B, arrows) consistent with a late stage of fusion or arrested dilation of nascent pores. C shows an enlarged region of B, which is reproduced in D with dashed white lines tracing the inferred position of each membrane. Dotted white lines indicate ambiguities, including places where the plane of the lipid bilayer was not perpendicular to the TEM section; such "slanted" membranes appear to split into two lines. (E–H) Antibody inhibition. Nuclei were assembled in the presence of (E) preimmune or (F–H) immune serum 3860 for 2 h. Positive control nuclei had typical nuclear envelopes with NPCs (E, arrows). Treatment with immune serum produced arrested electron-dense structures (F, arrows). G and H show an enlargement of two arrested nascent pores, with dashed white lines in H tracing the inferred position of each membrane. (I and J) Tangential section through mature NPC, with membranes traced by dashed white lines in J. Bars: (A, B, E, and F) 200 nm; (C, D, G, H, and J) 10 nm; (I) refer to bar in J.

the surface images shown in Fig. 5 (+ tail). We estimated that the frequency of mini-pores was lower in the SEM images, probably due to masking of smaller pores by the 2.5-nm layer of chromium.

Membranes arrested by anti-tail antibodies were pointy rather than parallel, and we were unable to trace membranes within the electron-dense gap (Fig. 6 H, white dotted lines). Few, if any, mini-pores were detected in antibody-arrested membranes by surface imaging (Fig. 5). Thus, exogenous tails and anti-tail antibodies produced subtly different arrest morphologies when viewed by TEM, independently supporting our surface imaging results. Antibodies appeared to inhibit either during or immediately after pore formation, whereas tail polypeptides appeared to inhibit later, during pore enlargement (dilation).

We next quantitated four definable morphological features in the TEM images (Fig. 7 A). These features were dimples (D), defined as short angular electron-dense indentations of the outer membrane; twinned (T) membranes, defined as ~40-nm paired indentations of the inner and outer membranes (originally described by Maul et al., 1971); mature NPCs (M); and both types of unusual arrested structures (A) (only the pointy structure is shown in Fig. 7 A). We counted these features, measured the total length (microns) of nuclear envelope examined (Fig. 7 B), and graphed their frequencies per micrometer of nuclear envelope (Fig. 7 C). This quantitation showed that mature NPCs were largely absent from the inhibited nuclei, strongly suggesting that gp210 is required for NPC formation. Few, if any, (0–5%) arrested structures were present in control nuclei, but comprised the majority (70%) of structures seen in tail- or antibody-arrested nuclei (Fig. 7 B). The slightly higher frequency of total pore-related structures in the inhibited nuclei (Fig. 7 B, structures/micrometer) suggested that these structures accumulated stably. Twinned membranes were relatively abundant in control nuclei (34–36% of total structures), but significantly reduced (to 2%) in tail-inhibited nuclei and reduced by half (to 15%) in antibody-inhibited nuclei. Similar structures, with closely-apposed inner and outer membranes, were shown by Maul et al. (1971) to be highly correlated with forming (or disassembling) pores. Because twinned membranes were abundant in our control nuclei, but missing or reduced in arrested nuclei, we suggest that the gp210 tail and its partners might trigger the close apposition of the inner and outer nuclear membranes in addition to mediating pore dilation.

Finally, we considered the possibility that our inhibitors might destabilize or revert mature NPCs, rather than (or in addition to) blocking de novo pore assembly. To test this model, we first preassembled nuclei for 90 min and then added 10 μM tail polypeptides, gp210 antibodies, or the

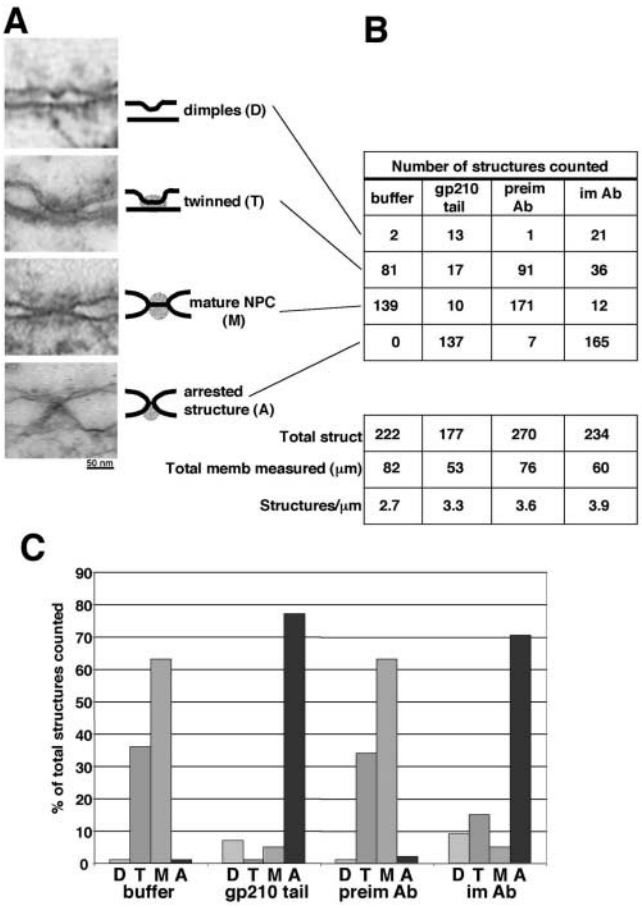

	Number of structures counted			
	buffer	gp210 tail	preim Ab	im Ab
	2	13	1	21
	81	17	91	36
	139	10	171	12
	0	137	7	165
Total struct	222	177	270	234
Total memb measured (μm)	82	53	76	60
Structures/μm	2.7	3.3	3.6	3.9

Figure 7. **Quantitation of pore-related nuclear membrane structures.** We (A) identified and (B) quantitated four morphological features termed dimples, twinned membranes, mature NPCs, and arrested structures on TEM micrographs of arrested and control nuclei. Results are graphed in C as the average number of each feature per micron for nuclei arrested by 10 μM gp210 tail (or buffer control), and for nuclei treated with preimmune (preimm) or immune (im) antibodies against the gp210 tail. For each positive control, the number (*n*) of individual nuclei from which these measurements were taken was 10; for tail polypeptide–inhibited nuclei, $n = 14$; for antibody-arrested nuclei, $n = 15$.

corresponding controls. We imaged these reactions by SEM immediately and 1 h later. The control and experimental nuclei all remained intact with mature NPCs and were indistinguishable by SEM (see Fig. S1, available at http://www.jcb.org/cgi/content/full/jcb.200108145/DC1), suggesting that our reagents did not grossly disrupt the structure or function of mature NPCs.

Discussion

We report the effects of two independent reagents that targeted the exposed cytosolic tail of gp210. Neither reagent affected NPC morphology when added to assembled nuclei. Importantly, neither reagent disrupted the membrane fusion events required to generate flattened nuclear membranes. However, when added to assembling nuclei, both reagents efficiently arrested nuclear pore formation at an early stage. To explain the mechanisms of arrest, we propose that exogenous tail polypeptides compete for tail-binding nucleoporins and block their binding to endogenous gp210. We propose that the anti-tail antibodies either cross-link endogenous gp210 tails and block their function sterically, or block their interactions with tail-binding partners, or both. The antibodies might arrest pore formation at a slightly earlier stage than exogenous/competing tail polypeptides. The antibody-arrested structures were electron dense, and individual membranes could not be traced, whereas polypeptide-inhibited membranes appeared to form narrow mini-pores 1–5 nm in diameter, which might permit limited diffusion. These tail-inhibited nuclei accumulated lamin B3 to low levels, consistent with (but not proving) the presence of narrow diffusion-competent pores. Structures consistent with tiny pores (~3–7-nm diameter) were also seen by surface imaging of tail-inhibited nuclear membranes. Importantly, our inhibitors also reduced the formation of closely-apposed twinned membranes, proposed by Maul et al. (1971) to be precursors to pore formation. These results strongly support our major conclusion that gp210 has early roles in nuclear pore formation.

Antibodies inhibited pore formation more severely than competing tails. When gp210 bound, these antibodies might interfere sterically with neighboring proteins that function independently of gp210. Alternatively, bound antibodies might cluster gp210 or induce other conformational changes that disrupt its lumenal domain. Antibodies that directly bind the lumenal domain of gp210 in vivo inhibit both active transport and passive diffusion (Greber and Gerace, 1992). We therefore speculate that our anti-tail antibodies might also functionally disrupt the lumenal domain of gp210.

Inhibitors have been useful to dissect the NPC assembly pathway. Two inhibitors, GTPγS and NEM, block the formation of fused, flattened membrane cisternae (Boman et al., 1992; Newport and Dunphy, 1992; Macaulay and Forbes, 1996). To study pore formation in vitro, one must start with fused flattened membranes. The fusion of nuclear/ER membranes involves the GTP-binding protein Ran (Hetzer et al., 2000; Zhang and Clarke, 2000) and p97 ATPase complexes (Hetzer et al., 2001). Nuclear membranes can self-assemble as stacks of flattened cisternae in the absence of chromatin (Dabauvalle et al., 1991; Meier et al., 1995). Membrane fusion is delayed by a Ca^{2+} buffer, BAPTA (Sullivan et al., 1993; Shumaker et al., 1998). BAPTA also completely blocks pore formation when added at time zero (Macaulay and Forbes, 1996), or causes "star ring" intermediates to accumulate if added later in assembly (Goldberg et al., 1997). Wheat germ agglutinin, a lectin that binds *O*-linked *N*-acetylglucosamine–modified nucleoporins, also blocks pore formation (Meier et al., 1995; Goldberg et al., 1997). Our present findings add two novel intermediates to the biochemically-defined pathway of pore formation. BAPTA-arrested nuclei have flattened parallel poreless membranes that lack FxFG repeat nucleoporins. In contrast, reagents that disrupt gp210 tail function appear to slow a proposed membrane apposition event before fusion, but then allow porogenic membrane fusion to initiate or progress to the mini-pore stage. We propose that the BAPTA-arrested and gp210 tail–arrested intermediates bracket the porogenic fusion event, providing direct experimental access to the mechanisms of pore formation and dilation.

Nucleoporin p62 may be recruited early during porogenesis

Gp210-arrested nuclei accumulated p62, but failed to accumulate nup214/CAN, nup98, or nup153. The p62 result was probably not an artifact, because we gradient purified our nuclei before running gels for Western blotting. There is currently no evidence that p62 binds directly to the gp210 tail. Thus, p62 might be recruited to nascent pores independent of gp210. The possible incorporation of p62 into gp210 tail–arrested nuclei is intriguing, because p62 and its binding partners form a ring structure (Macaulay and Forbes, 1995; Hu et al., 1996) and are critical for transport activity (Finlay et al., 1991).

Gp210 functions early in pore formation and its tail is involved in nuclear pore dilation

Our results suggest that interactions between the exposed tail of gp210 and its putative binding partners might trigger an important early event, namely the close apposition of inner and outer nuclear membranes before fusion. Although membrane fusion per se was not blocked, reagents that interfered with the gp210 tail or its putative partners also caused pore formation to arrest at two subsequent stages. For the antibody-arrested stage, we could not determine if membrane fusion was complete, due to the electron density of these pointy structures. However the mini-pores that accumulated in the presence of exogenous tail polypeptides appear to represent a normal intermediate in which the pore has formed, but cannot dilate. Based on previous SEM studies, nascent pores are thought to progressively increase in diameter from ~1–5 nm (dimples) to ~30–40 nm (stabilizing pores) and ~50–70 nm (mature pores; Maul, 1977; Goldberg et al., 1997). This model is supported by mini-pores, which have diameters of 3–7 nm when visualized by SEM and 1–5 nm when visualized by TEM. (Note that the 2.5-nm chromium coat on SEM samples would obscure pores <3 nm in diameter). Thus, our findings suggest direct roles for gp210 and its partners in triggering pore formation and dilating nascent pores. We speculate that soluble tail-binding nucleoporins play a positive role by forming spokes or struts between gp210 tails, which insertionally expand the size of the pore. Note that if tail-binding partners had inhibitory roles, pores would expand uncontrollably in the presence of competing gp210 tail polypeptides. We can therefore rule out inhibitory roles for tail-binding nucleoporins.

Pore dilation: a regulated event during nuclear pore formation?

Kozerski et al. (2000) proposed that the hydrophobicity of the tail domain of influenza HA is crucial for pore dilation, because dilation was blocked by a hydrophilic tail. The only known function of the HA tail is passive: to exist, and not interfere with fusion or pore dilation. Thus, the final diameter of the pore may be irrelevant to a virus. Gp210 tails from *Xenopus*, rat, and *Caenorhabditis elegans* also contain 30–45% hydrophobic residues, although their positions are not conserved. However, we conclude that the tail of gp210 is not passive, because our results suggest that nuclear pore dilation is coupled to the assembly of soluble nucleoporins. Without this link, NPCs might assemble incorrectly, or worse, pores themselves might enlarge and fenestrate the nuclear envelope, destroying its integrity as a boundary. Our results strongly suggest that the tail of gp210 plus one or more unidentified tail-binding nucleoporins mediate the close apposition of nuclear membranes, and nuclear pore dilation. Possible mechanisms to control pore dilation include the oligomerization of gp210 lumenal domains into a grommet that encircles the pore membrane domain, or the assembly of tail-binding struts, or both.

Nuclear membrane fusion and pore dilation could be coupled efficiently if the same protein (or two interacting proteins) mediated both events. Our results thus do not rule out, and moreover support, the hypothesis that gp210 directly mediates porogenic membrane fusion (Wozniak et al., 1989; Greber et al., 1990; Wozniak and Blobel, 1992). However, our results restrict the still hypothetical, fusogenic activity of gp210 to its highly-conserved lumenal domain (Cohen et al., 2001). Testing these models for gp210 function will require determining the gp210-null phenotype and identifying nucleoporins that bind its tail.

Materials and methods

Partial cDNA cloning of *Xenopus* gp210

We identified an 807-bp cDNA clone (AW642061) in the Blackshear/Soares normalized database for *Xenopus* egg library ESTs and obtained the EST clone from Research Genetics Inc. After sequencing this DNA, we compared its predicted ORF for the gp210 tail with rat gp210. The predicted Xgp210 tail had 23 fewer amino acids, due to an extra nucleotide that created a stop codon. To determine if this stop codon was a PCR artifact in the EST clone, we did a PCR reaction from a stage I/II *Xenopus* oocyte cDNA library (from A. Wolffe, National Institutes of Health, Bethesda, MD) using primers 5′-TGTAAAACGACGGCCAGT-3′ and 5′-CAGGAAACAGCTATGACC-3′. This partial cDNA was subcloned into the pCRT7 TOPO TA vector (Invitrogen) to generate clone Xp-gp210, which was DNA sequenced (unpublished data) and shown to lack the truncating mutation. The longer amino acid sequence predicted by our clone, Xp-gp210, is shown in Fig. 1.

Expression construct for GST–gp210 tail fusion

Different primers were used to generate a cDNA encoding only the cytoplasmic tail (COOH-terminal 61 residues) of *Xenopus* gp210 from the *Xenopus* stage I/II oocyte DNA library noted above. These new primers added BamH1 and Sma1 sites to the 5′ and 3′ regions of the gp210 tail, respectively (sense primer, 5′-GGGGCAGCAATAACCGGATCCATTATGTCA-3′; antisense primer, 5′-ACCCCAAATCCCGGGACAACATCGTTGTAC-3′). The PCR product and pGEX-2T vector (Amersham Pharmacia Biotech) were both sequentially digested with BamH1 and Sma1, gel purified, and ligated together. Correct insertion of the Gp210 tail fragment into pGEX-2T was verified by double-stranded DNA sequencing (unpublished data). The resulting construct, named *Xenopus* tail (Xt)-gp210, was expressed in bacteria as a recombinant protein consisting of the gp210 tail fused at its NH_2 terminus to GST.

Protein expression and thrombin cleavage

The pGEX-2T vector containing the gp210 tail insert was transformed into competent *Escherichia coli* cells (strain BL21 DE3 pLysS; Novagen, Inc.) and grown in LB media containing 40 μg/ml ampicillin and 36 μg/ml chloramphenicol to an OD_{600} of 0.5. Protein expression was induced for 3 h using 1 mM IPTG. Cells were pelleted and the fusion protein purified by chromatography on glutathione-Sepharose according to manufacturer specifications (Amersham Pharmacia Biotech). The purified fusion protein was incubated with biotin-conjugated thrombin (Novagen, Inc.) for 4 h at 22–24°C. Biotinylated thrombin was removed by binding to streptavidin-Sepharose (Novagen, Inc.). Isolated gp210 tail polypeptide was either used fresh or stored in aliquots at –20°C.

Antibodies

A peptide corresponding to the predicted COOH-terminal 16 residues of *Xenopus* gp210 (GSFYFQRLLYPNCPLV) was synthesized, purified by re-

verse phase HPLC with the use of a C18 analytical column, and conjugated to keyhole limpet hemocyanin by Boston Biomolecules. This peptide was used to immunize rabbit 3860. mAb 414, which is specific for FG repeat nucleoporins, was from Covance Research Products. The mAb against *Xenopus* lamin B3, 46F7, was the gift of Reimer Stick (Göttingen University, Göttingen, Germany). Rabbit serum 2806 was raised against recombinant *Xenopus* LAP2 residues 1–165, comprising the "constant" region of *Xenopus* LAP2 (Gant et al., 1999; Dechat et al., 2000). Rabbit serum production was done by Covance Research Products.

Nuclear assembly reactions

Demembranated *Xenopus* sperm chromatin (used at 1,000 sperm/μl extract) was prepared as previously described (Newmeyer and Wilson, 1991) and incubated at 22–24°C in reconstituted cell-free extracts of *Xenopus* eggs supplemented with 2 mM ATP, 10 mM creatine phosphate, and 50 μg/ml creatine kinase (Hutchison et al., 1988). Assembly reactions were then supplied with purified recombinant *Xenopus* gp210 tail, immune or preimmune serum 3860, or an equal volume of wash buffer (50 mM Hepes, pH 7.6, 50 mM KCl, 2.5 mM $MgCl_2$, 1 μg/ml leupeptin, 1 μg/ml aprotinin) as a control. These reagents contributed no more than 10% to the final volume.

Isolation of nuclei assembled in vitro

To isolate in vitro–assembled nuclei, 50-μl assembly reactions were diluted with 1 ml of ice-cold nuclear isolation buffer (NIB) (20 mM Tris-HCl, pH 7.4, 70 mM KCl, 5 mM $MgCl_2$, 2 mM DTT, 2% polyvinylpyrolidone). Diluted reactions were pooled and layered over 60% Percoll (in NIB) and centrifuged at 3,000 *g* for 10 min at 4°C. Material was collected from the NIB–Percoll interface, supplemented with ice-cold NIB to a volume of 1 ml, layered over 0.5 ml of 25% sucrose (wt/vol in NIB), and centrifuged at 2,500 rpm in a benchtop microfuge to yield a nuclear pellet. The nuclear pellet was resuspended in SDS sample buffer and boiled for 3 min. For analysis by SDS-PAGE and Western blotting, the equivalent of 2×10^5 nuclei was loaded per lane, as confirmed by removing an aliquot and counting the number of pelleted nuclei.

SDS-PAGE, immunoblotting, and densitometry

Proteins were resolved on precast 4–12% Bis-Tris polyacrylamide gels (Novex) by electrophoresis at 200 V for 1 h, and then either stained with Coomassie blue or transferred to a polyvinylidene difluoride membrane. Immunoblots were probed with a 1:500 dilution of anti-gp210 tail serum 3860 in PBS-T (PBS containing 0.1% Tween-20). Alternatively, blots were probed for 1 h at 22–24°C with (a) mAb 414 diluted to 1:5,000 with PBS-T or (b) monoclonal antibody 46F7 at a 1:500 dilution to detect *Xenopus* lamin B3. After three washes in PBS-T, blots were incubated for 1 h at 22–24°C with 1:25,000 dilution of HRP-conjugated secondary antibodies (anti–rabbit or anti–mouse; Pierce Chemical Co.). Membranes were washed as before and visualized by ECL (Amersham Pharmacia Biotech). To probe for LAP2, each blot was stripped by incubation with 15% H_2O_2 (in PBS) for 30 min at 22–24°C, washed for 15 min in PBS-T, incubated with serum 2806 diluted 1:50,000, and processed as described above. LAP2-probed blots were then restripped and blotted for gp210 as described above.

Fluorescence microscopy

Aliquots of assembly reactions were diluted fourfold with Fix-Stain buffer (15 mM Pipes, pH 7.2, 80 mM KCl, 5 mM EDTA, 15 mM NaCl, 3.3% formaldehyde, and 10 μg/ml Hoescht 33258). Samples were imaged on a Nikon Microphot using a cooled CCD camera with UV filters to detect DNA and phase contrast to visualize nuclear membranes. *Xenopus* A6 cells were cultured in a 60% solution of Leibovitz L15 media containing 10% FBS, MEM nonessential amino acid solution (1×), penicillin, and streptomycin (each at 0.1 mg/ml). Cells were fixed in PBS with 4% paraformaldehyde, and stained for indirect immunofluorescence using mAb 414 at 1:5,000, or serum 3860 at 1:100. Goat ant–rabbit secondary antibodies were conjugated with either Cy3 or FITC and used at 1:500. DNA was stained with Hoescht. Images were collected and processed using IPLab Spectrum software.

Field emission SEM

A 4-μl aliquot of each assembly reaction was diluted in 500 μl buffer (150 mM sucrose, 50 mM KCl, 2.5 mM $MgCl_2$, 50 mM Hepes, pH 8, 1 mM DTT, 1 μg/ml each of aprotinin and leupeptin) and sedimented at 3,000 *g* for 10 min at 4°C onto acetone-washed silicon chips (Fred Pella). Chips were incubated for at least 10 min in SEM fix buffer (150 mM sucrose, 50 mM KCl, 80 mM Pipes-KOH, pH 6.8, 1 mM $MgCl_2$, 0.25% gluteraldehyde (EM grade), 2% paraformaldehyde [Sigma-Aldrich]). Chips were then washed in 0.2 M sodium cacodylate, pH 7.2, post-fixed for 10 min in 1% OsO_4 (in 0.2 M Na cacodylate, pH 7.2), washed in water, stained for 10 min in 1% uranyl acetate (in water), and dehydrated in a graded ethanol series (30%, 50%, 70%, 95%, and two times at 100% ethanol, followed by two times at 100% Arklone). Samples were then critical point dried from high purity CO_2 using Arklone (trichlorotrifluoroethane; ICI) as a transitional solvent. Dried samples were sputter coated with a 2.5-nm coat of chromium in an Edwards Auto 306 coating unit. Samples were viewed on the top stage of an ABT dual stage SEM (DS-130F) (Topcon Corp.) at a 30-kV accelerating voltage.

TEM

Nuclear assembly reactions (50 μl) were diluted in 3% gluteraldehyde, 1.5% paraformaldehyde, 0.1 M sodium cacodylate, and 3 mM $MgCl_2$ to a final volume of 1 ml, and fixed for 1 h on ice. Nuclei were then pelleted in a Beckman Coulter Microfuge E horizontal benchtop centrifuge for 1 min at high speed at 4°C. Pellets were incubated on ice four times (10 min each) with 0.1 M sodium cacodylate and 3 mM $MgCl_2$, repelleted, and then incubated with 2% osmium tetroxide (in 0.1 M sodium cacodylate with 3 mM $MgCl_2$) for 1 h on ice. Pellets were washed twice with water (5 min each), incubated in 2% aqueous uranyl acetate at 22–24°C, and then dehydrated through a graded ethanol series (30, 50, 70, 95, 100%). After three 10-min incubations in 100% ethanol, samples were embedded in Spurrs, sectioned, and viewed on a Philips microscope at 60 kV.

Online supplemental material

Fig. S1 (available online at http://www.jcb.org/cgi/content/full/jcb.200108145/DC1) shows that exogenous gp210 tail polypeptides and anti-tail antibodies have no detectable effects on preformed NPCs. Nuclei were preassembled for 90 min, treated for 1 h with buffer or 10 μM tail polypeptide, or immune or preimmune serum 3860, and imaged by SEM.

We thank R. Stick for the antilamin antibody, and M. Matunis, C. Machamer, K.K. Lee, J. Cronshaw (Johns Hopkins University), Y. Gruenbaum, M. Cohen (Hebrew University of Jerusalem, Jerusalem, Israel), M. Zastrow (Johns Hopkins University), and an anonymous reviewer for interesting discussions or comments on the manuscript. We are grateful to S. Rutherford, M. Goldberg, and T. Allen (Paterson Institute, Manchester, England) for their help with SEM sample preparation and image collection.

This work was funded by a postdoctoral fellowship from the Wellcome Trust, UK (to S.P. Drummond), and a research grant from the National Institutes of Health (RO1-GM48646 to K.L. Wilson).

Submitted: 29 August 2001
Revised: 16 May 2002
Accepted: 20 May 2002

References

Aris, J.P., and G. Blobel. 1989. Yeast nuclear envelope proteins cross react with an antibody against mammalian pore complex proteins. *J. Cell Biol.* 108:2059–2067.

Bayliss, R., A.H. Corbett, and M. Stewart. 2000. The molecular mechanism of transport of macromolecules through nuclear pore complexes. *Traffic.* 1:448–456.

Bennet, M.K., and R.H. Scheller. 1993. The molecular machinery for secretion is conserved from yeast to neurons. *Proc. Natl. Acad. Sci. USA.* 90:2559–2563.

Bodoor, K., S. Shaikh, D. Salina, W.H. Raharjo, R. Bastos, M. Lohka, and B. Burke. 1999. Sequential recruitment of NPC proteins to the nuclear periphery at the end of mitosis. *J. Cell Sci.* 112:2253–2264.

Boman, A.L., M.R. Delannoy, and K.L. Wilson. 1992. GTP hydrolysis is required for vesicle fusion during nuclear envelope assembly in vitro. *J. Cell Biol.* 116: 281–294.

Chaudhary, N., and J.C. Courvalin. 1993. Stepwise reassembly of the nuclear envelope at the end of mitosis. *J. Cell Biol.* 122:295–306.

Cohen, M., K.L. Wilson, and Y. Gruenbaum. 2001. Membrane proteins of the nuclear pore complex: gp210 is conserved in *Drosophila, C. elegans* and *Arabidopsis. Gene Ther. Mol. Biol.* 6:47–55.

Dabauvalle, M.C., K. Loos, H. Merkert, and U. Scheer. 1991. Spontaneous assembly of pore complex–containing membranes ("annulate lamellae") in *Xenopus* egg extract in the absence of chromatin. *J. Cell Biol.* 112:1073–1082.

Daigle, N., J. Beaudouin, L. Hartnell, G. Imreh, E. Hallberg, J. Lippincott-Schwartz, and J. Ellenberg. 2001. Nuclear pore complexes form immobile

networks and have a very low turnover in live mammalian cells. *J. Cell Biol.* 154:71–84.

Davis, L.I., and G. Blobel. 1987. Nuclear pore complex contains a family of glycoproteins that includes p62: glycosylation through a previously unidentified cellular pathway. *Proc. Natl. Acad. Sci. USA.* 84:7552–7556.

Dechat, T., S. Vlcek, and R. Foisner. 2000. Lamina-associated polypeptide 2 isoforms and related proteins in cell cycle-dependent nuclear structure dynamics. *J. Struct. Biol.* 129:335–345.

Fabergé, A.C. 1974. The nuclear pore complex: its free existence and a hypothesis as to its origin. *Cell Tissue Res.* 151:403–415.

Favreau, C., H.J. Worman, R.W. Wozniak, T. Frappier, and J.C. Courvalin. 1996. Cell cycle-dependent phosphorylation of nucleoporins and nuclear pore membrane protein Gp210. *Biochemistry.* 35:8035–8044.

Favreau, C., R. Bastos, J. Cartaud, J.C. Courvalin, and P. Mustonen. 2001. Biochemical characterization of nuclear pore complex protein gp210 oligmers. *Eur. J. Biochem.* 268:3883–3889.

Finlay, D.R., E. Meier, P. Bradley, J. Horecka, and D.J. Forbes. 1991. A complex of nuclear pore proteins required for pore function. *J. Cell Biol.* 114:169–183.

Firmbach-Kraft, I., and R. Stick. 1995. Analysis of nuclear lamin isoprenylation in *Xenopus* oocytes: isoprenylation of lamin B3 precedes its uptake into the nucleus. *J. Cell Biol.* 129:17–24.

Fontoura, B.M., S. Dales, G. Blobel, and H. Zhong. 2001. The nucleoporin Nup98 associates with the intranuclear filamentous protein network of TPR. *Proc. Natl. Acad. Sci. USA.* 98:3208–3213.

Gajewski, A., D. Lourim, and G. Krohne. 1996. An antibody against a glycosylated integral membrane protein of the *Xenopus laevis* nuclear pore complex: a tool for the study of pore complex membranes. *Eur. J. Cell Biol.* 71:14–21.

Gant, T.M., C.A. Harris, and K.L. Wilson. 1999. Roles of LAP2 proteins in nuclear assembly and DNA replication: truncated LAP2β proteins alter lamina assembly, envelope formation, nuclear size, and DNA replication efficiency in *Xenopus laevis* extracts. *J. Cell Biol.* 144:1083–1096.

Gerace, L., Y. Ottaviano, and C. Kondor-Koch. 1982. Identification of a major polypeptide of the nuclear pore complex. *J. Cell Biol.* 95:826–837.

Goldberg, M.W., C. Wiese, T.D. Allen, and K.L. Wilson. 1997. Dimples, pores, star-rings, and thin rings on growing nuclear envelopes: evidence for structural intermediates in nuclear pore complex assembly. *J. Cell Sci.* 110:409–420.

Greber, U.F., and L. Gerace. 1992. Nuclear protein import is inhibited by an antibody to a lumenal epitope of a nuclear pore complex glycoprotein. *J. Cell Biol.* 116:15–30.

Greber, U.F., A. Senior, and L. Gerace. 1990. A major glycoprotein of the nuclear pore complex is a membrane-spanning polypeptide with a large lumenal domain and a small cytoplasmic tail. *EMBO J.* 9:1495–1502.

Haraguchi, T., T. Koujin, T. Hayakawa, T. Kaneda, C. Tsutsumi, N. Imamoto, C. Akazawa, J. Sukegawa, Y. Yoneda, and Y. Hiraoka. 2000. Live fluorescence imaging reveals early recruitment of emerin, LBR, RanBP2, and Nup153 to reforming functional nuclear envelopes. *J. Cell Sci.* 113:779–794.

Hernandez, L.D., L.R. Hoffman, T.G. Wolfsberg, and J.M. White. 1996. Virus-cell and cell-cell fusion. *Annu. Rev. Cell Dev. Biol.* 12:627–661.

Hetzer, M., D. Bilbao-Cortes, T.C. Walther, O.J. Gruss, and I.W. Mattaj. 2000. GTP hydrolysis by Ran is required for nuclear envelope assembly. *Mol. Cell.* 5:1013–1024.

Hetzer, M., H.H. Meyer, T.C. Walther, D. Bilbao-Cortes, G. Warren, and I.W. Mattaj. 2001. Distinct AAA-ATPase p97 complexes function in discrete steps of nuclear assembly. *Nat. Cell Biol.* 3:1086–1091.

Hu, T., T. Guan, and L. Gerace. 1996. Molecular and functional characterization of the p62 complex, an assembly of nuclear pore complex glycoproteins. *J. Cell Biol.* 134:589–601.

Hutchison, C.J., R. Cox, and C.C. Ford. 1988. The control of DNA replication in a cell-free extract that recapitulates a basic cell cycle in vitro. *Development.* 103:553–566.

Imreh, G., and E. Hallberg. 2000. An integral membrane protein from the nuclear pore complex is also present in the annulate lamellae: implications for annulate lamella formation. *Exp. Cell Res.* 259:180–190.

Kozerski, C., E. Ponimaskin, B. Schroth-Diez, M.F. Schmidt, and A. Herrmann. 2000. Modification of the cytoplasmic domain of influenza virus hemagglutinin affects enlargement of the fusion pore. *J. Virol.* 74:7529–7537.

Kraemer, D., R.W. Wozniak, G. Blobel, and A. Radu. 1994. The human CAN protein, a putative oncogene product associated with myeloid leukemogenesis, is a nuclear pore complex protein that faces the cytoplasm. *Proc. Natl. Acad. Sci. USA.* 91:1519–1523.

Loewinger, L., and F. McKeon. 1988. Mutations in the nuclear lamin proteins resulting in their aberrant assembly in the cytoplasm. *EMBO J.* 7:2301–2309.

Lohka, M.J., and Y. Masui. 1984. Roles of cytoplasmic particles in nuclear envelope assembly and sperm pronuclear formation in cell-free preparations from amphibian eggs. *J. Cell Biol.* 98:1222–1230.

Macaulay, C., and D.J. Forbes. 1995. Differential mitotic phosphorylation of proteins of the nuclear pore complex. *J. Biol. Chem.* 270:254–262.

Macaulay, C., and D.J. Forbes. 1996. Assembly of the nuclear pore: biochemically distinct steps revealed with NEM, GTPγS, and BAPTA. *J. Cell Biol.* 132:5–20.

Marelli, M., C.P. Lusk, H. Chan, J.D. Aitchison, and R.W. Woziak. 2001. A link between the synthesis of nucleoporins and the biogenesis of the nuclear envelope. *J. Cell Biol.* 153:709–724.

Maul, G.G. 1977. The nuclear and the cytoplasmic pore complex: structure, dynamics, distribution, and evolution. *Int. Rev. Cytol. Suppl.* 6:75–186.

Maul, G.G., J.W. Price, and M.W. Lieberman. 1971. Formation and distribution of nuclear pore complexes in interphase. *J. Cell Biol.* 51:405–418.

Meier, E., B.R. Miller, and D.J. Forbes. 1995. Nuclear pore complex assembly studied with a biochemical assay for annulate lamellae formation. *J. Cell Biol.* 129:1459–1472.

Meier, J., K.H. Campbell, C.C. Ford, R. Stick, and C.J. Hutchison. 1991. The role of lamin LIII in nuclear assembly and DNA replication, in cell-free extracts of *Xenopus* eggs. *J. Cell Sci.* 98:271–279.

Miller, B.R., and D.J. Forbes. 2000. Purification of the vertebrate nuclear pore complex by biochemical criteria. *Traffic.* 1:941–951.

Newmeyer, D.D., and K.L. Wilson. 1991. Egg extracts for nuclear import and nuclear assembly reactions. *Methods Cell Biol.* 36:607–634.

Newport, J.W., and W.G. Dunphy. 1992. Characterization of the membrane binding and fusion events during nuclear envelope assembly using purified components. *J. Cell Biol.* 116:295–306.

Panté, N., and U. Aebi. 1994. Toward the molecular details of the nuclear pore complex. *J. Struct. Biol.* 113:179–189.

Radu, A., M.S. Moore, and G. Blobel. 1995. The peptide repeat domain of nucleoporin Nup98 functions as a docking site in transport across the nuclear pore complex. *Cell.* 81:215–222.

Reichelt, R., A. Holzenburg, E.L. Buhle, Jr., M. Jarnik, A. Engel, and U. Aebi. 1990. Correlation between structure and mass distribution of the nuclear pore complex and of distinct pore complex components. *J. Cell Biol.* 110:883–894.

Robinson, L.J., and T.F. Martin. 1998. Docking and fusion in neurosecretion. *Curr. Opin. Cell Biol.* 10:483–492.

Shah, S., and D.J. Forbes. 1998. Separate nuclear import pathways converge on the nucleoporin Nup153 and can be dissected with dominant-negative inhibitors. *Curr. Biol.* 8:1376–1386.

Shumaker, D.K., L.R. Vann, M.W. Goldberg, T.D. Allen, and K.L. Wilson. 1998. TPEN, a Zn^{2+}/Fe^{2+} chelator with low affinity for Ca^{2+}, inhibits lamin assembly, stabilizes nuclear architecture and may independently protect nuclei from apoptosis in vitro. *Cell Calcium.* 23:151–164.

Skehel, J.J., and D.C. Wiley. 2000. Receptor binding and membrane fusion in virus entry: the influenza hemagglutinin. *Annu. Rev. Biochem.* 69:531–569.

Soderqvist, H., and E. Hallberg. 1994. The large C-terminal region of the integral pore membrane protein, POM121, is facing the nuclear pore complex. *Eur. J. Cell Biol.* 64:186–191.

Sullivan, K.M., W.B. Busa, and K.L. Wilson. 1993. Calcium mobilization is required for nuclear vesicle fusion in vitro: implications for membrane traffic and IP3 receptor function. *Cell.* 73:1411–1422.

Sukegawa, J., and G. Blobel. 1993. A nuclear pore complex protein that contains zinc finger motifs, binds DNA, and faces the nucleoplasm. *Cell.* 72:29–38.

Vasu, S.K., and D.J. Forbes. 2001. Nuclear pores and nuclear assembly. *Curr. Opin. Cell Biol.* 13:363–375.

Wente, S.R. 2000. Gatekeepers of the nucleus. *Science.* 288:1374–1377.

Wiese, C., M.W. Goldberg, T.D. Allen, and K.L. Wilson. 1997. Nuclear envelope assembly in *Xenopus* extracts visualized by scanning EM reveals a transport-dependent "envelope smoothing" event. *J. Cell Sci.* 110:1489–1502.

Wozniak, R.W., and G. Blobel. 1992. The single transmembrane segment of gp210 is sufficient for sorting to the pore membrane domain of the nuclear envelope. *J. Cell Biol.* 119:1441–1449.

Wozniak, R.W., E. Bartnik, and G. Blobel. 1989. Primary structure analysis of an integral membrane glycoprotein of the nuclear pore. *J. Cell Biol.* 108:2083–2092.

Yoneda, Y. 2000. Nucleocytoplasmic protein traffic and its significance to cell function. *Genes Cells.* 5:777–787.

Zhang, C., and P.R. Clarke. 2000. Chromatin-independent nuclear envelope assembly induced by Ran GTPase in *Xenopus* egg extracts. *Science.* 288:1429–1432.